Report

Luminal Cells Are Favored as the Cell of Origin for Prostate Cancer

Zhu A. Wang,[1,3] Roxanne Toivanen,[1] Sarah K. Bergren,[1] Pierre Chambon,[2] and Michael M. Shen[1,*]

[1]Departments of Medicine, Genetics and Development, Urology, and Systems Biology, Columbia Stem Cell Initiative, Herbert Irving Comprehensive Cancer Center, Columbia University College of Physicians and Surgeons, New York, NY 10032, USA
[2]Institut de Génétique et de Biologie Moléculaire et Cellulaire, CNRS UMR7104, INSERM U964, 67400 Illkirch, France
[3]Present address: Department of Molecular, Cell and Developmental Biology, University of California, Santa Cruz, Santa Cruz, CA 95064, USA
*Correspondence: mshen@columbia.edu

SUMMARY

The identification of cell types of origin for cancer has important implications for tumor stratification and personalized treatment. For prostate cancer, the cell of origin has been intensively studied, but it has remained unclear whether basal or luminal epithelial cells, or both, represent cells of origin under physiological conditions in vivo. Here, we use a novel lineage-tracing strategy to assess the cell of origin in a diverse range of mouse models, including $Nkx3.1^{+/-}$; $Pten^{+/-}$, $Pten^{+/-}$, Hi-Myc, and $TRAMP$ mice, as well as a hormonal carcinogenesis model. Our results show that luminal cells are consistently the observed cell of origin for each model in situ; however, explanted basal cells from these mice can generate tumors in grafts. Consequently, we propose that luminal cells are favored as cells of origin in many contexts, whereas basal cells only give rise to tumors after differentiation into luminal cells.

INTRODUCTION

The identification of cell types of origin for cancer is significant, since distinct cell populations within a tissue may give rise to different cancer subtypes distinguished by their histopathological phenotypes and patient outcomes (Blanpain, 2013; Visvader, 2009, 2011; Wang et al., 2013). Numerous studies have investigated the cell of origin by introducing an oncogenic insult within a defined cell type to determine whether these cells can give rise to cancer. However, such approaches are potentially limited, as the cell type of origin may be dependent on the specific oncogenic insult and/or the model system. To date, no studies have systematically addressed which cell types can serve as cells of origin in multiple contexts of tumor initiation.

In human and mouse prostate epithelium, luminal and basal cells are the two major cell types, together with rare neuroendocrine cells (Shen and Abate-Shen, 2010). Lineage tracing has shown that luminal and basal cells in the adult mouse prostate represent distinct populations that are mostly self-sustaining (Choi et al., 2012; Lu et al., 2013; Wang et al., 2013). Notably,

lineage-marked basal cells rarely generate luminal cells during adult tissue homeostasis but display plasticity under the influence of inductive embryonic urogenital mesenchyme in grafting assays, acquiring facultative progenitor properties and generating luminal cells (Choi et al., 2012; Lu et al., 2013; Wang et al., 2013).

For prostate cancer, previous studies have reached differing conclusions regarding the cell type(s) of origin (Goldstein and Witte, 2013; Wang and Shen, 2011; Xin, 2013). Although prostate adenocarcinoma has a luminal phenotype, both basal and luminal cells have been proposed to represent cells of origin. In particular, transformed human basal cells can give rise to prostate cancer in renal grafting models (Goldstein et al., 2010; Stoyanova et al., 2013; Taylor et al., 2012), whereas a luminal stem cell population identified in the regressed mouse prostate can act as a cell of origin in vivo (Wang et al., 2009). More recently, lineage tracing in mice in which the $Pten$ tumor suppressor was specifically deleted in either basal or luminal cells has shown that both cell types can act as cells of origin (Choi et al., 2012; Lu et al., 2013; Wang et al., 2013).

However, it remains unclear whether basal or luminal cells, or both, represent cell types of origin in the context of $Pten$ deletion occurring throughout the prostate epithelium or whether the cell of origin might vary depending upon specific oncogenic events. We have investigated this issue using a novel lineage-tracing strategy in a diverse range of mouse models that recapitulate important features of human prostate tumorigenesis. Our results indicate that luminal cells are consistently favored as cells of origin for prostate cancer.

RESULTS

To determine the cell of origin for a mouse model of prostate cancer, we performed lineage marking of either basal or luminal cells in apparently normal tissue to determine whether their progeny contribute to the tumors that subsequently arise (Figure 1). Since the lineage-tracing methodology uses inducible Cre recombinase, we analyzed mouse models in which the tumor phenotype is not driven by Cre. We used the $CK5$-$CreER^{T2}$ driver (Rock et al., 2009) for lineage tracing of basal cells and the PSA-$CreER^{T2}$ (Ratnacaram et al., 2008) or $CK8$-$CreER^{T2}$ (Van Keymeulen et al., 2011) drivers for tracing of luminal cells, together with the $R26R$-YFP reporter (Srinivas et al., 2001). Tamoxifen
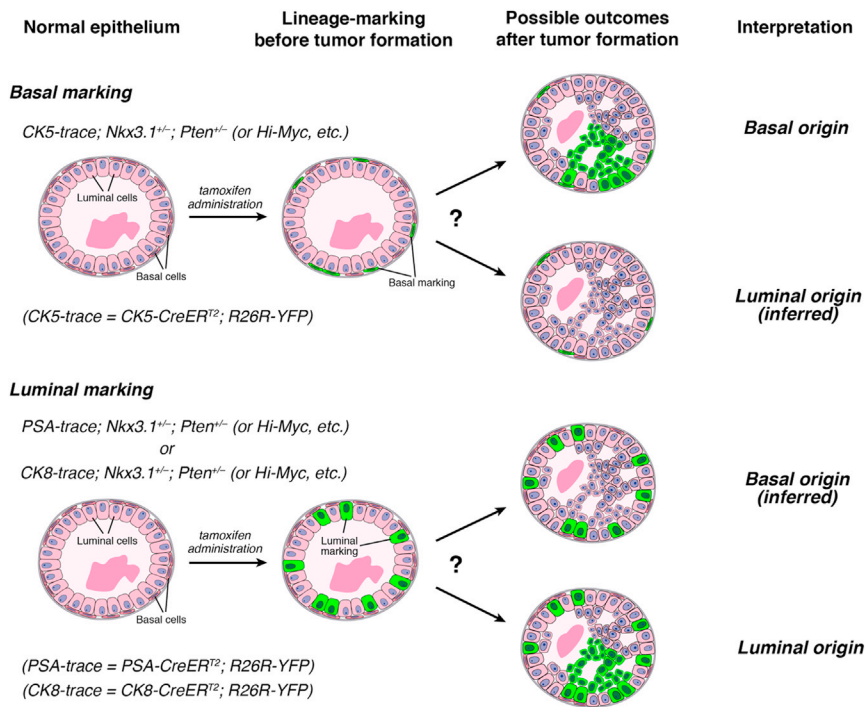
Figure 1. Experimental Design for Analysis of Cell of Origin

The inducible $CK5\text{-}CreER^{T2}$ driver can lineage mark basal cells by YFP expression in different prostate cancer models prior to overt cancer formation. Similarly, the inducible $PSA\text{-}CreER^{T2}$ and $CK8\text{-}CreER^{T2}$ drivers can mark luminal cells in phenotypically normal epithelium. The presence of YFP+ cell clusters in subsequent PIN/cancer lesions indicates that the marked cell type acts as the cell of origin in the mouse model analyzed.

induction for lineage marking was performed in young adult male mice at 7 weeks of age, when the basal and luminal lineages have been established as largely self-sustaining compartments (Choi et al., 2012; Ousset et al., 2012; Wang et al., 2013). Contribution of cells marked by the $CK5\text{-}CreER^{T2}$ driver to tumors would imply that basal cells were the cell of origin, whereas tumor cells marked by the $PSA\text{-}CreER^{T2}$ or $CK8\text{-}CreER^{T2}$ drivers would indicate a luminal origin (Figure 1). Notably, our approach dissociates the time of lineage marking from the onset of tumorigenesis and allows multiple models to be analyzed using the same overall strategy.

In control experiments to examine the specificity of the inducible Cre drivers in a wild-type background, we found that $CK5\text{-}CreER^{T2}; R26R\text{-}YFP$ (which we denote CK5-trace) strictly marks basal cells with 23.6% efficiency, while $PSA\text{-}CreER^{T2}; R26R\text{-}YFP$ (PSA-trace) marks luminal cells with 11.5% efficiency and $CK8\text{-}CreER^{T2}; R26R\text{-}YFP$ (CK8-trace) marks 4.1% of luminal cells (Tables S1L, S1N, and S1P), consistent with previous studies (Ousset et al., 2012; Ratnacaram et al., 2008; Wang et al., 2013). Importantly, the percentage of lineage-marked cells in the CK5-trace and PSA-trace mice does not change between 2 months of age, shortly after labeling, and 6 months of age, when most of our tumor analyses are mostly performed (Figure S1; Tables S2A and S2B), indicating that the lineage-marked cell populations are stable in a nontumorigenic background.

We first investigated the cell of origin for the high-grade prostatic intraepithelial neoplasia (PIN) lesions in the $Nkx3.1^{+/-}; Pten^{+/-}$ (which we denote NP) model that is heterozygous for null alleles of the Nkx3.1 homeobox gene and of Pten (Kim et al., 2002). As reported previously, the anterior prostate (AP) and dorsolateral prostate (DLP) of NP mice appear normal at 2 months of age (Figures 2E and 2J) but frequently display high-grade PIN/carcinoma lesions at 6 months (Figures 2F and 2K). Quantitation of initial lineage marking in CK5-trace; NP mice and PSA-trace; NP mice revealed similar efficiencies as mice with a wild-type background (Figures 2B, 2C, and 2Y; Tables S1A and S1B). Notably, in tumor lesions of CK5-trace; NP mice at 6 months of age, we found that yellow fluorescent protein (YFP)+ cells in clusters (defined as containing at least three YFP+ cells) were rarely observed (0.5%, n = 6 mice) (Figures 2G, 2L, and 2Y; Figures S2A and S2D; Table S1A), while the percentage of YFP+ cells in untransformed regions was unaffected (Figures S3A–S3C; Table S2C). In contrast, 10.8% of the cells in the tumor lesions of PSA-trace; NP mice (n = 4) and 4.5% of the cells in tumor lesions of CK8-trace; NP mice (n = 3) were YFP+ (Figures 2H, 2I, 2M, 2N, and 2Y; Figures S2B, S2C, S2E, and S2F; Tables S1B, S1C, and S1P). Furthermore, we found that YFP+ clusters were also rare in PIN lesions of 6-month-old CK5-trace; $Pten^{+/-}$ mice, whereas the frequency of YFP+ cells was unchanged in nontumor regions (n = 3) (Figures S3D, S3E, S4A, S4B, S4D, S4E, and S4G; Tables S1D and S2D). However, the percentage of YFP+ cells in PIN lesions of PSA-trace; $Pten^{+/-}$ mice (n = 3) was similar to the percentage initially marked by the $PSA\text{-}CreER^{T2}$ inducible driver (Figures S4C, S4F, and S4G; Table S1E).

Next, we examined the transgenic $ARR_2/probasin\text{-}Myc$ (Hi-Myc) model, in which expression of c-Myc is driven in both luminal and basal compartments, leading to invasive adenocarcinoma (Ellwood-Yen et al., 2003). Consistent with previous studies (Ellwood-Yen et al., 2003), the histology of the AP in Hi-Myc mice was mostly normal at 2 months of age (Figure 2O), although the DLP and ventral prostate (VP) were hyperplastic (Figures S4H and S4K). In the PIN/carcinoma lesions in the AP of CK5-trace; Hi-Myc mice at 6 months, YFP+ cell clusters were rare, whereas the percentage of YFP+ basal cells in untransformed regions was unaffected (n = 5 mice) (Figures 2P, 2Q, and 2Z; Figures S2G, S3F, and S3G; Tables S1F and S2E). In contrast, 13.1% of the cells within the PIN/carcinoma lesions of 6-month-old PSA-trace; Hi-Myc mice (n = 6) were YFP+, similar to the initial percentage (12.6%) of luminal cells marked at 2 months (Figures 2R and 2Z; Figure S2H; Table S1G). Similarly, YFP+ cells were present in PIN/carcinoma lesions of
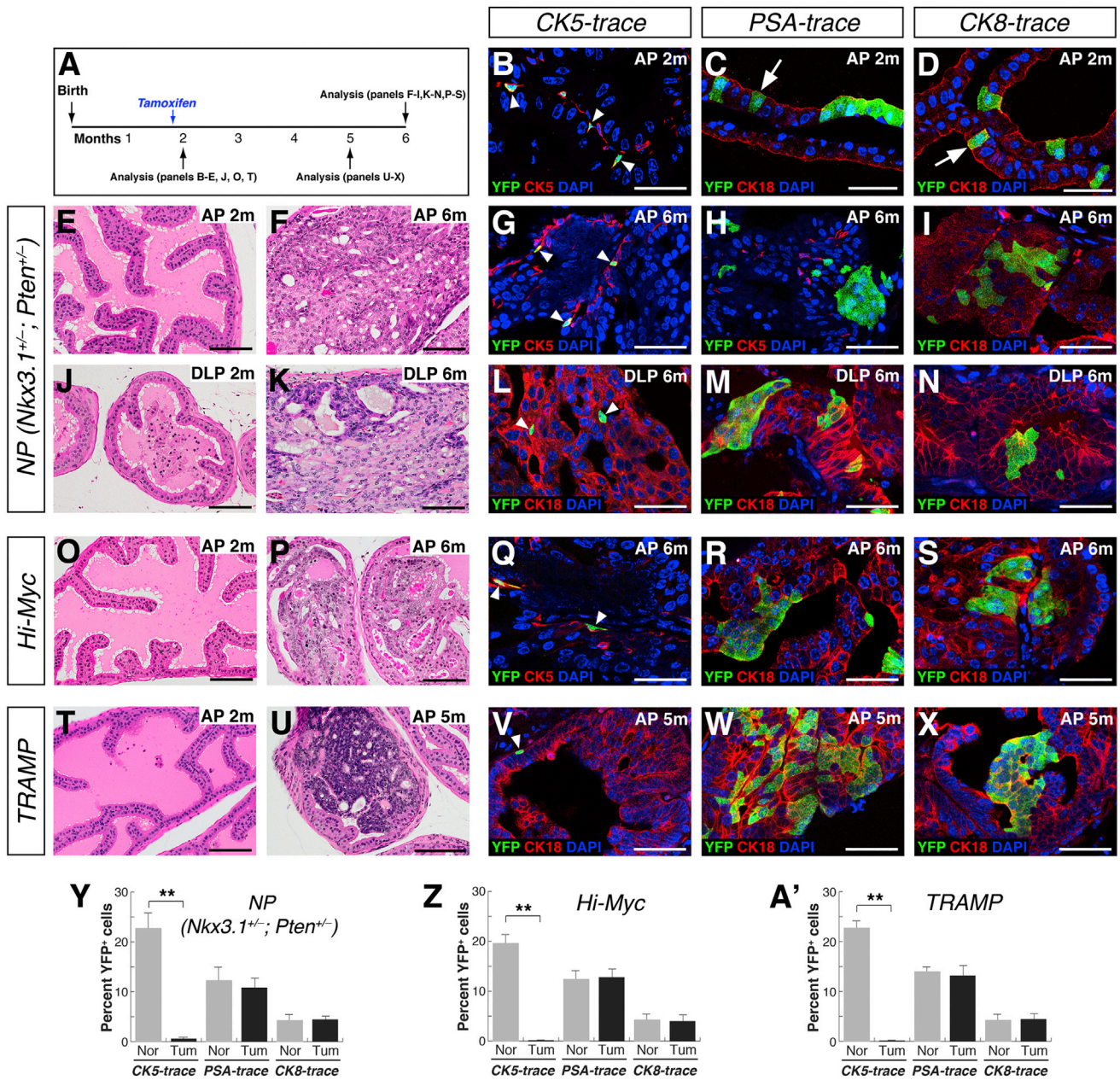
Figure 2. Luminal Cells Are Favored Cells of Origin in the *NP, Hi-Myc,* and *TRAMP* Models

(A) Experimental time course.

(B) Lineage marking of basal cells (arrowheads) in the AP of *CK5-trace; NP* mice at 2 months of age.

(C and D) Marking of luminal cells (arrows) in the AP of *PSA-trace; NP* mice (C) or *CK8-trace* mice (D) at 2 months.

(E, F, J, and K) H&E staining of *NP* prostates shows normal histology at 2 months and PIN/carcinoma lesions at 6 months.

(G and L) Clusters of YFP^{+} cells are rarely detected in *CK5-trace; NP* tumor lesions at 6 months.

(H, I, M, and N) YFP[+] cell clusters in tumor lesions of *PSA-trace; NP* (H and M) and *CK8-trace; NP* (I and N) mice at 6 months.

(O and P) Normal AP histology in *Hi-Myc* mice at 2 months (O) and PIN/carcinoma lesions at 6 months (P).

(Q) Absence of YFP[+] cell clusters in *CK5-trace; Hi-Myc* tumor lesions in the AP at 6 months.

(R and S) YFP[+] cell clusters in tumor lesions of *PSA-trace; Hi-Myc* mice (R) and *CK8-trace; Hi-Myc* mice (S) at 6 months.

(T and U) Normal histology of the AP in *TRAMP* mice at 2 months (T) and carcinoma at 5 months (U).

(V) Absence of YFP[+] cell clusters in *CK5-trace; TRAMP* AP tumor lesions at 5 months.

(W and X) YFP[+] clusters in AP tumor lesions of *PSA-trace; TRAMP* (W) and *CK8-trace; TRAMP* (X) mice at 5 months.

(Y–A′) Percentage of YFP^{+} cells in *NP* (Y), *Hi-Myc* (Z), and *TRAMP* (A′) models; Nor = normal, Tum = tumor; **p < 0.001 by Student's t test; error bars are 1 SD.
Arrowheads in (G), (L), (Q), and (V) indicate marked basal cells. Scale bars correspond to 50 μm in (B)–(D), (G)–(I), (L)–(N), (Q)–(S), and (V)–(X) and 100 μm in (E), (F), (J), (K), (O), (P), (T), and (U). See also Figures S1–S4.

CK8-trace; Hi-Myc mice (n = 4) in proportion to the initial luminal marking efficiency (Figures 2S and 2Z; Figure S2I; Tables S1H and S1P). Similar results were found in the DLP and VP of CK5-trace; Hi-Myc and PSA-trace; Hi-Myc mice (Figures S4H–S4M).

We also investigated the TRAMP model, which expresses the SV40 large T antigen under the control of the probasin promoter, giving rise to aggressive tumors (Greenberg et al., 1995). We found that the AP in TRAMP mice appeared mostly normal at 2 months but developed invasive, poorly differentiated adeno-carcinoma by 5 months (Figures 2T and 2U). In tumor lesions of CK5-trace; TRAMP mice (n = 4), YFP+ cell clusters were not observed, whereas the frequency of YFP+ cells in nontumor regions was unaffected (Figures 2V and 2A′; Figures S2J, S3H, and S3I; Tables S1I and S2F). However, YFP+ cell clusters were found in tumor lesions of PSA-trace; TRAMP mice (n = 5) and CK8-trace; TRAMP mice (n = 3) in percentages similar to the initial luminal marking efficiencies (Figures 2W, 2X, and 2A′; Figures S2K and S2L; Tables S1J, S1K, and S1P). Similar results were observed in the DLP and VP of TRAMP mice, although these lobes were already hyperplastic at 2 months of age (Figures S4N–S4S). Taken together, these findings show that luminal cells are the favored cell of origin in each of the genetically engineered mouse models examined.

Given the potential caveat that cancer initiation might occur prior to adulthood in these genetically engineered models, we investigated the cell of origin in a hormonal carcinogenesis paradigm (Ricke et al., 2008; Wang et al., 2000), in which lineage marking unequivocally takes place prior to prostate tumor initiation (Bosland et al., 1995; Noble, 1977; Ricke et al., 2008; Wang et al., 2000). After lineage marking of basal cells in CK5-trace mice or luminal cells in PSA-trace and CK8-trace mice (Figures 3A–3D; Tables S1L, S1N, and S1P), we treated the mice with a combination of testosterone (T) and estradiol-17β (E2) for 4 months, resulting in formation of low-grade PIN lesions in all prostate lobes (Figures 3E, 3I, and 3M). Using this protocol, we found that YFP+ clusters were rare in PIN lesions of CK5-trace mice (n = 5), while the frequency of YFP+ cells was unaffected in untransformed regions (Figures 3F, 3J, 3N, and 3Q; Figures S2M, S2P, S2S, S3J, and S3K; Tables S1M and S2G). In contrast, YFP+ clusters were present in PIN lesions of PSA-trace (n = 4) and CK8-trace mice (n = 3) (Figures 3G, 3H, 3K, 3L, 3O, 3P; Figures S2N, S2O, S2Q, S2R, S2T, and S2U), with the percentage of YFP+ cells similar to the initial efficiency of luminal cell marking (Figure 3Q; Tables S1O and S1Q). These results indicate that carcinogenesis induced by T+E2 treatment leads to prostate cancer initiation from luminal cells.

Previous studies have concluded that basal cells are cells of origin for human prostate cancer using renal grafting methods (Goldstein et al., 2010; Stoyanova et al., 2013; Taylor et al., 2012). To determine whether the potential discrepancy between these studies and our findings might be due to the different methodologies employed, we tested whether basal cells in our mouse models of prostate cancer could give rise to tumors after renal grafting. We performed tamoxifen induction of CK5-trace; Hi-Myc mice at 7 weeks of age and isolated basal cells by flow sorting for YFP (Figures 4A and 4B). The sorted basal cells were recombined with rat urogenital sinus mesenchyme and

grafted under the renal capsule of immunodeficient NOD.Cg-Prkdc^scid Il2rg^tm1Sug/JicTac (NOG) mice, followed by analysis after 3 months (Figure 4C). We observed extensive regions of YFP+ epithelium, which contained PIN lesions that were mostly composed of luminal cells, indicating that basal to luminal differentiation had taken place (Figures 4D–4F). We obtained similar results for basal cells isolated from CK5-trace; TRAMP mice (Figures 4G–4I), as well as from CK5-trace; Pten^+/− mice, in which the graft PIN lesions were also positive for phospho-Akt (Figures 4J–4L). Finally, we performed renal grafting of YFP+ basal cells isolated from tamoxifen-induced CK5-trace mice, followed by treatment of the NOG graft recipients with T+E2 for 3 months (Figure 4M). In the resulting grafts, marked basal cells could give rise to PIN lesions that mostly contained luminal cells (Figures 4N and 4O). Taken together, our results show that prostate basal cells are not favored as the cell of origin in their native microenvironment for any of the mouse models analyzed but nonetheless can give rise to tumors in renal grafts.

DISCUSSION

In principle, the cell of origin for cancer might be context specific, depending upon the oncogenic pathways being activated. In our studies, we have employed a novel lineage-tracing methodology for systematic assessment of the cell of origin for prostate cancer in a diverse range of mouse models. Using this "agnostic" lineage-tracing approach, we have unexpectedly found that luminal epithelial cells are consistently observed as the cell of origin.

Overall, we have analyzed a representative sample of widely used mouse models of human prostate cancer (Irshad and Abate-Shen, 2013; Ittmann et al., 2013; Shappell et al., 2004). However, there may be specific caveats associated with each model; for example, tumor initiation might conceivably occur in basal cells prior to 7 weeks of age in the transgenic models, resulting in early basal-to-luminal differentiation that would escape lineage marking. This possibility seems unlikely, since all tumor initiation would have to occur prior to 7 weeks of age to avoid detection of subsequent tumor formation from basal cells by lineage tracing. Nonetheless, our analysis has yielded the remarkably consistent result that luminal cells are favored as the cell of origin, and consequently we believe that this finding is likely to reflect the biology of prostate cancer, rather than a coincidence of intrinsic biases in each model. However, we note that basal cells could nonetheless act as cells of origin for prostate adenocarcinoma in other experimental contexts. In addition, the ability of inflammation to enhance basal-to-luminal differentiation in vivo (Kwon et al., 2014) suggests that alterations of the tissue microenvironment could influence the cell of origin (Goldstein and Witte, 2013).

To date, the cell of origin has usually been assayed by conditional gene targeting to generate oncogenic insults within a specific cell type. However, if the targeted cell type is a stem/progenitor cell, it can be difficult to discern whether tumor initiation takes place within the stem/progenitor itself or instead within its differentiated progeny. In this situation, it can be useful to distinguish between a "cell of origin" and a "cell of mutation" as distinct entities (Liu et al., 2011; Liu and Zong, 2012). In
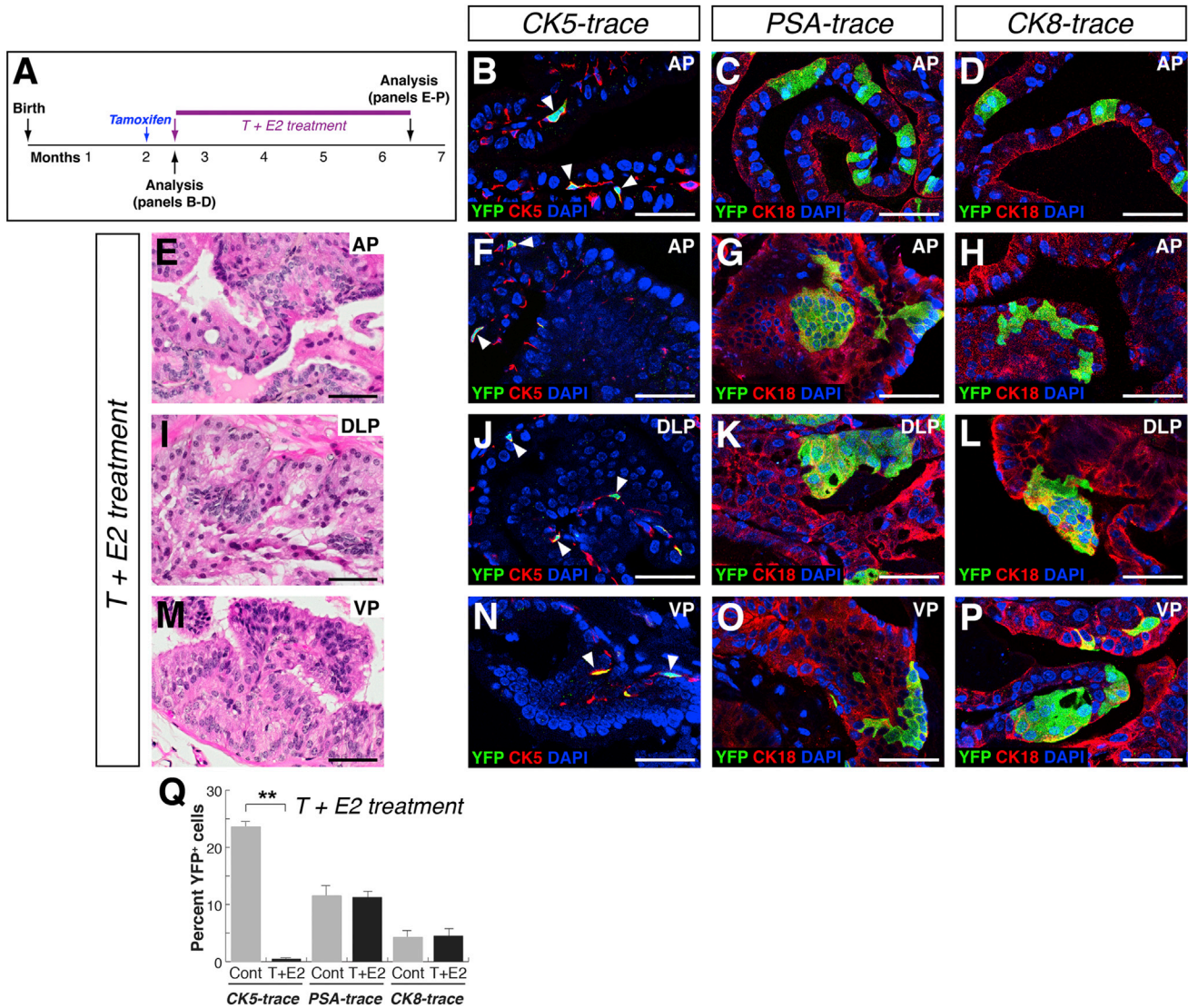
Figure 3. Luminal Cells Are the Favored Cell of Origin of Tumors Induced by T+E2 Hormonal Treatment
(A) Experimental time course.
(B–D) Lineage marking of basal (arrowheads) and luminal cells in control *CK5-trace* (B), *PSA-trace* (C), and *CK8-trace* (D) mice.
(E, I, and M) PIN lesions in mice after T+E2 treatment.
(F, J, and N) YFP$^+$ cell clusters are rarely detected in *CK5-trace* PIN lesions after T+E2 treatment; arrowheads indicate marked basal cells.
(G, H, K, L, O, and P) YFP$^+$ clusters in PIN lesions of *PSA-trace* (G, K, O) and *CK8-trace* (H, L, P) mice after T+E2 treatment.
(Q) Percentage of YFP$^+$ cells. Cont, control untreated; T+E2, treated. **p < 0.001 by Student's t test. Error bars are 1 SD.
Scale bars indicate 50 μm. See also Figures S2 and S3.

particular, a progenitor that initially acquires a mutation may not directly transform and hence be a "cell of mutation," while its lineage-restricted progeny may inherit the mutation and subsequently undergo oncogenic transformation and thus would represent a "cell of origin." For example, lineage tracing of gliomas in a *p53; Nf1* mouse model has shown that neural stem cells act as a cell of mutation, whereas their descendant oligodendrocyte progenitors correspond to the cell of origin (Liu et al., 2011).

In this regard, prostate basal cells removed from their normal tissue microenvironment can acquire facultative bipotential pro-

genitor properties after combination with embryonic urogenital mesenchyme, resulting in the differentiation of luminal cells (Goldstein et al., 2008; Lawson et al., 2007, 2010; Wang et al., 2013), while transformed basal cells give rise to luminal tumors in renal grafts (Goldstein et al., 2010; Stoyanova et al., 2013; Taylor et al., 2012). Our findings are consistent, since lineage-marked basal cells in each of our mouse models can give rise to prostate cancer in the context of renal grafts. Consequently, we propose that mutated basal cells do not usually act as a cell of origin in prostate tissue in situ but can function as a cell of mutation in renal grafts by acquiring facultative progenitor
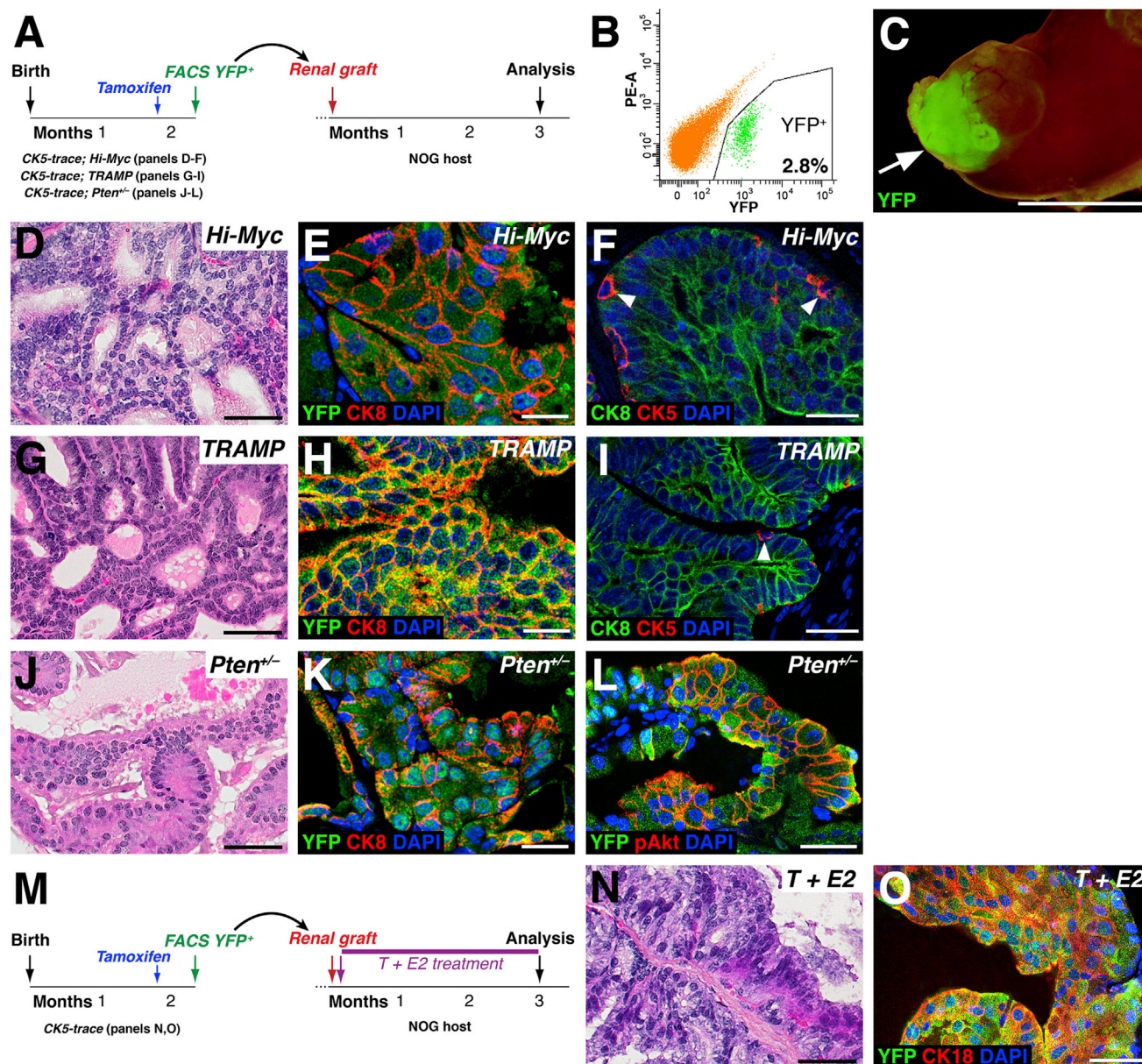
Figure 4. Basal Cells Can Give Rise to Prostate Cancer in Renal Grafts

(A) Experimental design.

(B) Representative flow-sort of YFP⁺ basal cells (2.8% of total prostate cells) from *CK5-trace; Hi-Myc* mice.

(C) Kidney from recipient NOG mouse containing graft with YFP fluorescence (arrow).

(D–I) Grafted basal cells from *CK5-trace; Hi-Myc* (D–F) or *CK5-trace; TRAMP* (G–I) mice generate PIN lesions (D and G), which contain mostly luminal cells (E and H) and some basal cells (arrowheads, F and I).

(J–L) Basal cells from *CK5-trace; Pten*⁺ᐟ⁻ mice generate PIN lesions (J) that contain mostly luminal cells (K) and express phospho-Akt (L).

(M) Experimental design for T+E2 treatment of grafts.

(N and O) Grafted basal cells give rise to PIN lesions (N) that contain mostly luminal cells (O) after T+E2 treatment.

Scale bars correspond to 25 μm in (E), (F), (H), (I), and (K), 5 mm in (C), and 50 μm in (D), (G), (J), (N), and (O).

properties and thereby generating luminal progeny that are authentic cells of origin.

Notably, previous studies have shown that targeted deletion of *Pten* in basal cells results in formation of tumors in situ, albeit with a temporal delay that appears to be associated with

basal-to-luminal differentiation, and which are less aggressive than tumors arising from targeting of luminal cells (Choi et al., 2012; Wang et al., 2013). Interestingly, PIN lesions arose from targeted basal cells by 3 months of age, in contrast with the absence of contribution from lineage-marked basal cells in *NP*

and *Pten*^{+/−} mice. These findings are potentially consistent with a "competition" model, which is not mutually exclusive with the cell of mutation model. Thus, if *Pten* loss occurs in both luminal and basal cells, transformed luminal cells might emerge before basal cells can be transformed, and might suppress subsequent basal cell transformation in a non-cell-autonomous manner.

Finally, our finding that luminal cells are the favored cell of origin in multiple mouse models raises the possibility that most human prostate adenocarcinomas arise from luminal cells. In particular, cytological examination of human PIN lesions suggests that early initiating events occur in luminal cells, including c-Myc upregulation and telomere elongation (Gurel et al., 2008; Meeker et al., 2002). Moreover, human prostate luminal cells may be prone to cancer initiation due to a decreased DNA damage response (Jäämaa et al., 2010). Our results also imply that cell of origin analyses for human cancer may be inherently difficult using grafting assays, due to the plasticity of basal cells. Instead, approaches such as retrospective lineage tracing using mitochondrial mutations may provide insight into human prostate cancer origins (Blackwood et al., 2011; Gaisa et al., 2011). Since the cell of origin may be a critical factor in conferring aggressiveness in prostate cancer (Wang et al., 2013), these and other approaches to identify cell types of origin are likely to be important for biomarker identification and disease prognosis.

EXPERIMENTAL PROCEDURES

Mouse Procedures

Mouse lines were maintained on an inbred C57BL/6N or mixed C57BL/6N-129S6/SvEvTac background. Primer sequences for genotyping are listed in Table S2. For tamoxifen induction, mice were administered 9 mg/40 g tamoxifen (Sigma) suspended in corn oil by oral gavage once daily for 4 consecutive days.

For T+E2 treatment, a 1.0 cm Silastic capsule (No. 602–305 Silastic tubing; 1.54 mm inside diameter, 3.18 mm outside diameter; Dow-Corning #2415569) filled with testosterone (Sigma) and a 0.4 cm Silastic capsule filled with estradiol-17β (Sigma) were implanted subcutaneously. Mice were treated with hormones for 4 months.

All animal studies were performed using protocols approved by the Institutional Animal Care and Use Committee of Columbia University Medical Center.

Tissue Collection and Flow Cytometry

Prostate tissue dissection, fixation, and dissociation were performed as described previously (Wang et al., 2013). Cell sorting was performed based on YFP fluorescence on a BD FACS Aria II instrument in the Flow Cytometry Shared Resource of the Herbert Irving Comprehensive Cancer Center. We used side scatter/forward scatter gating to exclude debris and doublets, followed by phycoerythrin/YFP fluorescein isothiocyanate A gating to exclude autofluorescent double-positive cells and to collect the single-positive YFP-expressing cell population.

Renal Grafting Assay

For tissue recombinants, 1.0×10^4 dissociated YFP^{+} cells were mixed with 2.5×10^5 dissociated urogenital sinus mesenchyme cells from embryonic day 18.0 rat embryos. Tissue recombinants were cultured in Dulbecco's modified Eagle's medium/10% fetal bovine serum/10^{-7} M dihydrotestosterone overnight, followed by transplantation under the kidney capsules of immunodeficient NOD.Cg-*Prkdc*[scid] *Il2rg*[tm1Sug]/JicTac (NOG) mice (Taconic) and growth for 12 weeks.

Histology and Immunostaining

Hematoxylin and eosin (H&E) staining and immunofluorescence staining were performed (Wang et al., 2013) using the following primary antibodies: rabbit CK5 (Covance #PRB-160P, 1:1,000), rabbit CK8 (Abcam #ab53280, 1:250), mouse CK18 (Abcam #ab668, 1:100), chick GFP (Abcam #ab13970, 1:2,000), and rabbit phospho-Akt (Cell Signaling #3787, 1:50). Samples were incubated with secondary antibodies (diluted 1:500 in PBST) labeled with Alexa 488, Alexa Fluor 555, or Alexa Fluor 647 (Invitrogen/Molecular Probes) and mounted with VECTASHIELD medium with DAPI (Vector Labs). Immunofluorescence was imaged using a Leica TCS SP5 spectral confocal microscope.

Data Quantitation

Cell numbers were counted using confocal ×40 and ×63 photomicrographs. For histologically normal tissues at 2 months, the percentage of YFP^{+} cells (labeled "Nor" in Figures 2Y–2A' and S1G and "Cont" in Figure 3Q) represents the ratio of YFP^{+} cells to total basal or luminal cells. For tumor tissues at later ages, the percentage of YFP^{+} cells (labeled "Tum" in Figures 2Y–2A' and S1G and "T+E2" in Figure 3Q) represents the ratio of clustered YFP^{+} cells in tumor lesions to total epithelial cells within these lesions. Statistical analyses were performed using a two-sample t test. At least three animals for each experiment or genotype were analyzed.

SUPPLEMENTAL INFORMATION

Supplemental Information includes four figures and three tables and can be found with this article online at http://dx.doi.org/10.1016/j.celrep.2014.08.002.

AUTHOR CONTRIBUTIONS

Z.A.W. and M.M.S. designed the study. Z.A.W. performed the experiments, with contributions from R.T. for H&E and immunostaining, and S.K.B. for renal grafting. P.C. provided *PSA-CreER*[T2] mice. Z.A.W., R.T., and M.M.S. analyzed data and prepared the manuscript.

ACKNOWLEDGMENTS

REFERENCES

Blackwood, J.K., Williamson, S.C., Greaves, L.C., Wilson, L., Rigas, A.C., Sandher, R., Pickard, R.S., Robson, C.N., Turnbull, D.M., Taylor, R.W., and Heer, R. (2011). In situ lineage tracking of human prostatic epithelial stem cell fate reveals a common clonal origin for basal and luminal cells. J. Pathol. *225*, 181–188.

Blanpain, C. (2013). Tracing the cellular origin of cancer. Nat. Cell Biol. *15*, 126–134.

Bosland, M.C., Ford, H., and Horton, L. (1995). Induction at high incidence of ductal prostate adenocarcinomas in NBL/Cr and Sprague-Dawley Hsd:SD rats treated with a combination of testosterone and estradiol-17 beta or diethylstilbestrol. Carcinogenesis *16*, 1311–1317.

Choi, N., Zhang, B., Zhang, L., Ittmann, M., and Xin, L. (2012). Adult murine prostate basal and luminal cells are self-sustained lineages that can both serve as targets for prostate cancer initiation. Cancer Cell *21*, 253–265.

Ellwood-Yen, K., Graeber, T.G., Wongvipat, J., Iruela-Arispe, M.L., Zhang, J., Matusik, R., Thomas, G.V., and Sawyers, C.L. (2003). Myc-driven murine prostate cancer shares molecular features with human prostate tumors. Cancer Cell *4*, 223–238.

Gaisa, N.T., Graham, T.A., McDonald, S.A., Poulsom, R., Heidenreich, A., Jakse, G., Knuechel, R., and Wright, N.A. (2011). Clonal architecture of human prostatic epithelium in benign and malignant conditions. J. Pathol. *225*, 172–180.

Goldstein, A.S., and Witte, O.N. (2013). Does the microenvironment influence the cell types of origin for prostate cancer? Genes Dev. *27*, 1539–1544.

Goldstein, A.S., Lawson, D.A., Cheng, D., Sun, W., Garraway, I.P., and Witte, O.N. (2008). Trop2 identifies a subpopulation of murine and human prostate basal cells with stem cell characteristics. Proc. Natl. Acad. Sci. USA *105*, 20882–20887.

Goldstein, A.S., Huang, J., Guo, C., Garraway, I.P., and Witte, O.N. (2010). Identification of a cell of origin for human prostate cancer. Science *329*, 568–571.

Greenberg, N.M., DeMayo, F., Finegold, M.J., Medina, D., Tilley, W.D., Aspinall, J.O., Cunha, G.R., Donjacour, A.A., Matusik, R.J., and Rosen, J.M. (1995). Prostate cancer in a transgenic mouse. Proc. Natl. Acad. Sci. USA *92*, 3439–3443.

Gurel, B., Iwata, T., Koh, C.M., Jenkins, R.B., Lan, F., Van Dang, C., Hicks, J.L., Morgan, J., Cornish, T.C., Sutcliffe, S., et al. (2008). Nuclear MYC protein overexpression is an early alteration in human prostate carcinogenesis. Mod. Pathol. *21*, 1156–1167.

Irshad, S., and Abate-Shen, C. (2013). Modeling prostate cancer in mice: something old, something new, something premalignant, something metastatic. Cancer Metastasis Rev. *32*, 109–122.

Ittmann, M., Huang, J., Radaelli, E., Martin, P., Signoretti, S., Sullivan, R., Simons, B.W., Ward, J.M., Robinson, B.D., Chu, G.C., et al. (2013). Animal models of human prostate cancer: the consensus report of the New York meeting of the Mouse Models of Human Cancers Consortium Prostate Pathology Committee. Cancer Res. *73*, 2718–2736.

Jäämaa, S., Af Hällström, T.M., Sankila, A., Rantanen, V., Koistinen, H., Stenman, U.H., Zhang, Z., Yang, Z., De Marzo, A.M., Taari, K., et al. (2010). DNA damage recognition via activated ATM and p53 pathway in nonproliferating human prostate tissue. Cancer Res. *70*, 8630–8641.

Kim, M.J., Cardiff, R.D., Desai, N., Banach-Petrosky, W., Parsons, R., Shen, M.M., and Abate-Shen, C. (2002). Cooperativity of Nkx3.1 and Pten loss of function in a mouse model of prostate carcinogenesis. Proc. Natl. Acad. Sci. USA *99*, 2884–2889.

Kwon, O.J., Zhang, L., Ittmann, M.M., and Xin, L. (2014). Prostatic inflammation enhances basal-to-luminal differentiation and accelerates initiation of prostate cancer with a basal cell origin. Proc. Natl. Acad. Sci. USA *111*, E592–E600.

Lawson, D.A., Xin, L., Lukacs, R.U., Cheng, D., and Witte, O.N. (2007). Isolation and functional characterization of murine prostate stem cells. Proc. Natl. Acad. Sci. USA *104*, 181–186.

Lawson, D.A., Zong, Y., Memarzadeh, S., Xin, L., Huang, J., and Witte, O.N. (2010). Basal epithelial stem cells are efficient targets for prostate cancer initiation. Proc. Natl. Acad. Sci. USA *107*, 2610–2615.

Liu, C., and Zong, H. (2012). Developmental origins of brain tumors. Curr. Opin. Neurobiol. *22*, 844–849.

Liu, C., Sage, J.C., Miller, M.R., Verhaak, R.G., Hippenmeyer, S., Vogel, H., Foreman, O., Bronson, R.T., Nishiyama, A., Luo, L., and Zong, H. (2011). Mosaic analysis with double markers reveals tumor cell of origin in glioma. Cell *146*, 209–221.

Lu, T.L., Huang, Y.F., You, L.R., Chao, N.C., Su, F.Y., Chang, J.L., and Chen, C.M. (2013). Conditionally ablated Pten in prostate basal cells promotes basal-to-luminal differentiation and causes invasive prostate cancer in mice. Am. J. Pathol. *182*, 975–991.

Meeker, A.K., Hicks, J.L., Platz, E.A., March, G.E., Bennett, C.J., Delannoy, M.J., and De Marzo, A.M. (2002). Telomere shortening is an early somatic DNA alteration in human prostate tumorigenesis. Cancer Res. *62*, 6405–6409.

Noble, R.L. (1977). The development of prostatic adenocarcinoma in Nb rats following prolonged sex hormone administration. Cancer Res. *37*, 1929–1933.

Ousset, M., Van Keymeulen, A., Bouvencourt, G., Sharma, N., Achouri, Y., Simons, B.D., and Blanpain, C. (2012). Multipotent and unipotent progenitors contribute to prostate postnatal development. Nat. Cell Biol. *14*, 1131–1138.

Ratnacaram, C.K., Teletin, M., Jiang, M., Meng, X., Chambon, P., and Metzger, D. (2008). Temporally controlled ablation of PTEN in adult mouse prostate epithelium generates a model of invasive prostatic adenocarcinoma. Proc. Natl. Acad. Sci. USA *105*, 2521–2526.

Ricke, W.A., McPherson, S.J., Bianco, J.J., Cunha, G.R., Wang, Y., and Risbridger, G.P. (2008). Prostatic hormonal carcinogenesis is mediated by in situ estrogen production and estrogen receptor alpha signaling. FASEB J. *22*, 1512–1520.

Rock, J.R., Onaitis, M.W., Rawlins, E.L., Lu, Y., Clark, C.P., Xue, Y., Randell, S.H., and Hogan, B.L. (2009). Basal cells as stem cells of the mouse trachea and human airway epithelium. Proc. Natl. Acad. Sci. USA *106*, 12771–12775.

Shappell, S.B., Thomas, G.V., Roberts, R.L., Herbert, R., Ittmann, M.M., Rubin, M.A., Humphrey, P.A., Sundberg, J.P., Rozengurt, N., Barrios, R., et al. (2004). Prostate pathology of genetically engineered mice: definitions and classification. The consensus report from the Bar Harbor meeting of the Mouse Models of Human Cancer Consortium Prostate Pathology Committee. Cancer Res. *64*, 2270–2305.

Shen, M.M., and Abate-Shen, C. (2010). Molecular genetics of prostate cancer: new prospects for old challenges. Genes Dev. *24*, 1967–2000.

Srinivas, S., Watanabe, T., Lin, C.S., William, C.M., Tanabe, Y., Jessell, T.M., and Costantini, F. (2001). Cre reporter strains produced by targeted insertion of EYFP and ECFP into the ROSA26 locus. BMC Dev. Biol. *1*, 4.

Stoyanova, T., Cooper, A.R., Drake, J.M., Liu, X., Armstrong, A.J., Pienta, K.J., Zhang, H., Kohn, D.B., Huang, J., Witte, O.N., and Goldstein, A.S. (2013). Prostate cancer originating in basal cells progresses to adenocarcinoma propagated by luminal-like cells. Proc. Natl. Acad. Sci. USA *110*, 20111–20116.

Taylor, R.A., Toivanen, R., Frydenberg, M., Pedersen, J., Harewood, L., Collins, A.T., Maitland, N.J., and Risbridger, G.P.; Australian Prostate Cancer Bioresource (2012). Human epithelial basal cells are cells of origin of prostate cancer, independent of CD133 status. Stem Cells *30*, 1087–1096.

Van Keymeulen, A., Rocha, A.S., Ousset, M., Beck, B., Bouvencourt, G., Rock, J., Sharma, N., Dekoninck, S., and Blanpain, C. (2011). Distinct stem cells contribute to mammary gland development and maintenance. Nature *479*, 189–193.

Visvader, J.E. (2009). Keeping abreast of the mammary epithelial hierarchy and breast tumorigenesis. Genes Dev. *23*, 2563–2577.

Visvader, J.E. (2011). Cells of origin in cancer. Nature *469*, 314–322.

Wang, Z.A., and Shen, M.M. (2011). Revisiting the concept of cancer stem cells in prostate cancer. Oncogene *30*, 1261–1271.

Wang, Y., Hayward, S.W., Donjacour, A.A., Young, P., Jacks, T., Sage, J., Dahiya, R., Cardiff, R.D., Day, M.L., and Cunha, G.R. (2000). Sex hormone-induced carcinogenesis in Rb-deficient prostate tissue. Cancer Res. *60*, 6008–6017.

Wang, X., Kruithof-de Julio, M., Economides, K.D., Walker, D., Yu, H., Halili, M.V., Hu, Y.-P., Price, S.M., Abate-Shen, C., and Shen, M.M. (2009). A luminal epithelial stem cell that is a cell of origin for prostate cancer. Nature *461*, 495–500.

Wang, Z.A., Mitrofanova, A., Bergren, S.K., Abate-Shen, C., Cardiff, R.D., Califano, A., and Shen, M.M. (2013). Lineage analysis of basal epithelial cells reveals their unexpected plasticity and supports a cell-of-origin model for prostate cancer heterogeneity. Nat. Cell Biol. *15*, 274–283.

Xin, L. (2013). Cells of origin for cancer: an updated view from prostate cancer. Oncogene *32*, 3655–3663.